Electronic Supplementary Information for

Magnesium Amino-bis(phenolato) Complexes for the Ring-opening Polymerization of *rac*-Lactide

Katalin Devaine-Pressing,[a] Joshua H. Lehr,[a] Michelle E. Pratt,[a] Louise N. Dawe,[a,b] Amy A. Sarjeant,[c] and Christopher M. Kozak*,[a]

[a] Department of Chemistry, Memorial University of Newfoundland, St. John's, Newfoundland, Canada A1B 3X7. E-mail: ckozak@mun.ca; Tel: +1-709-864-8082
[b] C-CART X-ray Diffraction Laboratory, Memorial University of Newfoundland, St. John's, Newfoundland, Canada, Current Address: Department of Chemistry, Wilfrid Laurier University, Waterloo, Ontario, Canada
[c] Department of Chemistry, Northwestern University, 2145 Sheridan Rd. Evanston IL 60208

X-ray crystallography

Crystallographic and structure refinement data are given in Table S1. A single crystal of **2** was mounted on a glass fibre using Paratone-N oil. All measurements were made on a Rigaku Saturn CCD area detector with graphite monochromated Mo-K radiation solved on an AFC8-Saturn 70 single crystal X-ray diffractometer from Rigaku, equipped with an X-stream 2000 low temperature system. Using Olex2 [1], the structure was solved with the ShelXT [2] structure solution program using Direct Methods and refined with the ShelXL [3] refinement package using Least Squares minimisation.

Raw data images from the diffraction experiment were converted from Rigaku format to Bruker format via the program Eclipse (Parsons, Simon. 2010. ECLIPSE – Program for masking high pressure diffraction images and conversion between CCD image formats) for inspection, integration and scaling using APEX2 software (Bruker (2007). APEX2. Bruker AXS Inc., Madison, Wisconsin, USA.) The program Cell Now (Sheldrick, G. M. (2004). CELL NOW. University of Göttingen, Germany) was used to search for twin domains and returned four twin orientations. Upon inspection of the raw data frames it was determined that these four orientations were not twin domains but rather represented four unique orientations of the crystal for each run of the data collection. This is consistent with reports that the diffractometer used for data collection experienced slippage of the χ axis during data collections, resulting in shifting crystal orientation relative to the goniometer zeroes. Two of the orientations were similar enough that those two runs (Runs 1 and 3) could be integrated using the same orientation matrix. The other two runs were integrated separately, each with its own orientation matrix. After integration, the refined unit cell used for Runs 1 and 3 was used as the true unit cell. All four runs were scaled and corrected for absorption together using the program SADABS (Bruker (2001). SADABS. Bruker AXS Inc., Madison, Wisconsin, USA) to produce a merged, scaled HKLF file which was used for structure solution.

H-atoms were introduced in calculated positions, and refined on a riding model. All non-hydrogen atoms were refined anisotropically. One of the *t*-butyl groups was disordered with two orientations. These were refined as PARTs witth PART 1 = C26-C28 (and corresponding H-atoms) with occupancy = 0.508(8); PART 2 = C29-C31 (and corresponding H-atoms) with occupancy = 0.492(8). Distance and anisotropic restraings (RIGU and SADI) were applied to this group.

The OLEX2 [1] solvent masking routine was applied to recover 56.6 electrons per unit cell in two voids. An area of disperse electron density appeared to be present prior to the solvent masking, however, a good point atom model could not be achieved for this, and the content was not accounted for in the formula (or resulting intensive properties). The application of the solvent mask gave a good improvement in the data statistics and allowed for a full anisotropic refinement of the framework structure.

References:

1. Dolomanov, O.V., Bourhis, L.J., Gildea, R.J, Howard, J.A.K. & Puschmann, H. (2009), J. Appl. Cryst. 42, 339-341.
2. Sheldrick, G.M. (2015). Acta Cryst. A71, 3-8.
3. Sheldrick, G.M. (2008). Acta Cryst. A64, 112-122.

Table S1. Crystallographic and structure refinement data for **2**

Compound	**2**
Empirical formula	$C_{56}H_{84}Mg_2N_4O_4$
Formula weight	925.89
Temperature/K	163(2)
Crystal system	monoclinic
Space group	C2/c
a/Å	31.345(14)
b/Å	9.706(5)
c/Å	25.551(12)
α/°	90
β/°	113.998(14)
γ/°	90
Volume/Å^3	7102(6)
Z	4
ρ_{calc}g/cm^3	0.866
μ/mm^{-1}	0.070
F(000)	2016.0
Crystal size/mm^3	0.20 × 0.20 × 0.20
Radiation	MoKα (λ = 0.71073)
2Θ range for data collection/°	4.432 to 52.876
Index ranges	$-38 \le h \le 38$, $-12 \le k \le 10$, $-31 \le l \le 31$
Reflections collected	31988
Independent reflections	7246 [R_{int} = 0.0748, R_{sigma} = 0.0820]
Data/restraints/parameters	7246/15/339
Goodness-of-fit on F^2	0.985
Final R indexes [I>=2σ (I)]	R_1 = 0.0784, wR_2 = 0.2128
Final R indexes [all data]	R_1 = 0.1222, wR_2 = 0.2416
Largest diff. peak/hole / e Å^{-3}	0.41/-0.38
CCDC Reference Number	1043113

[a] $R_1 = \Sigma(||F_o| - |F_c||)/ \Sigma|F_o|)$; $wR_2 = [\Sigma(w(F_o^2 - F_c^2)^2)/ \Sigma w(F_o^2)^2]^{1/2}$.

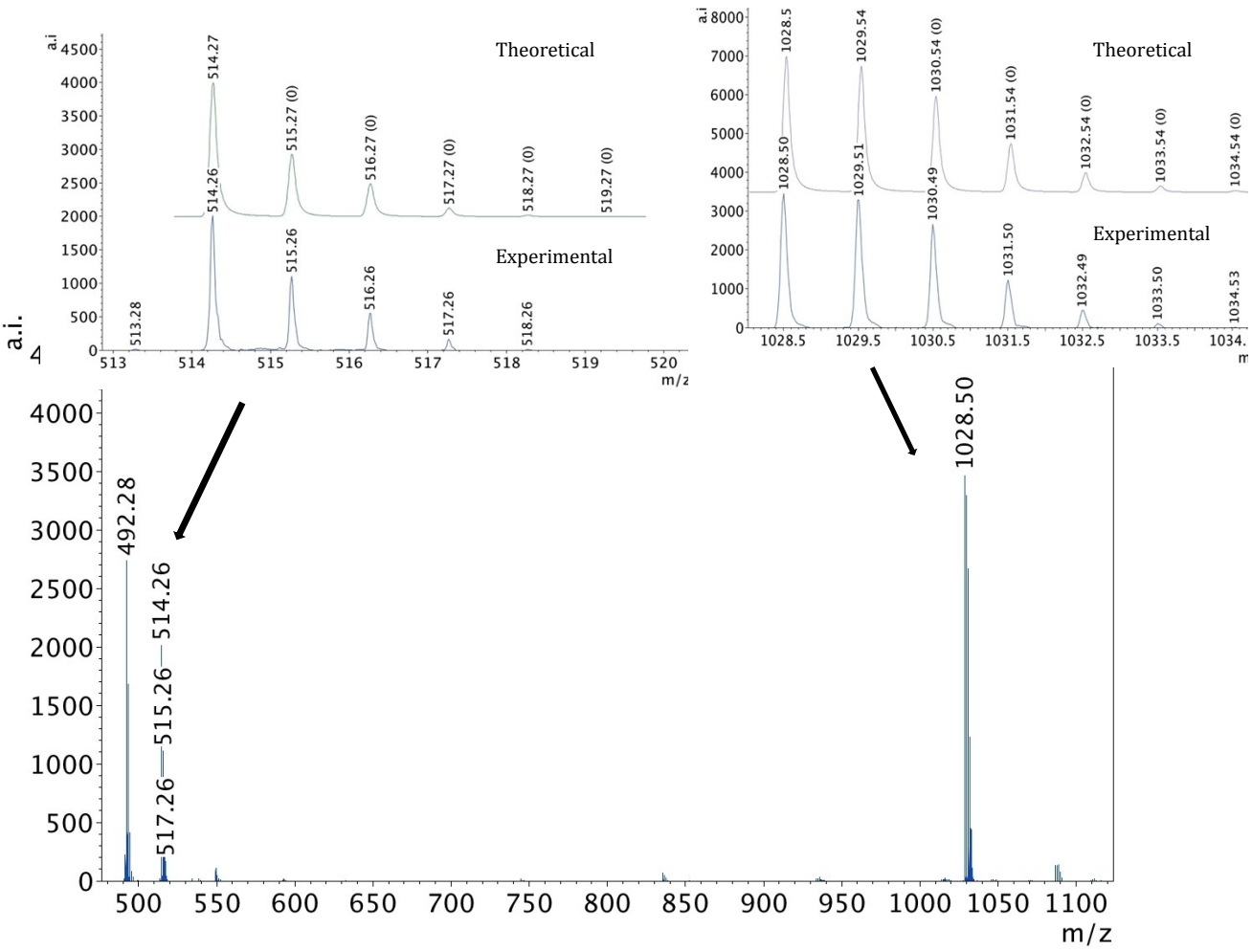

Fig. S1. MALDI-TOF mass spectrum of complex **1** with theoretical and experimental representation of the isotopic distribution pattern of both the monomer and the dimer ions.

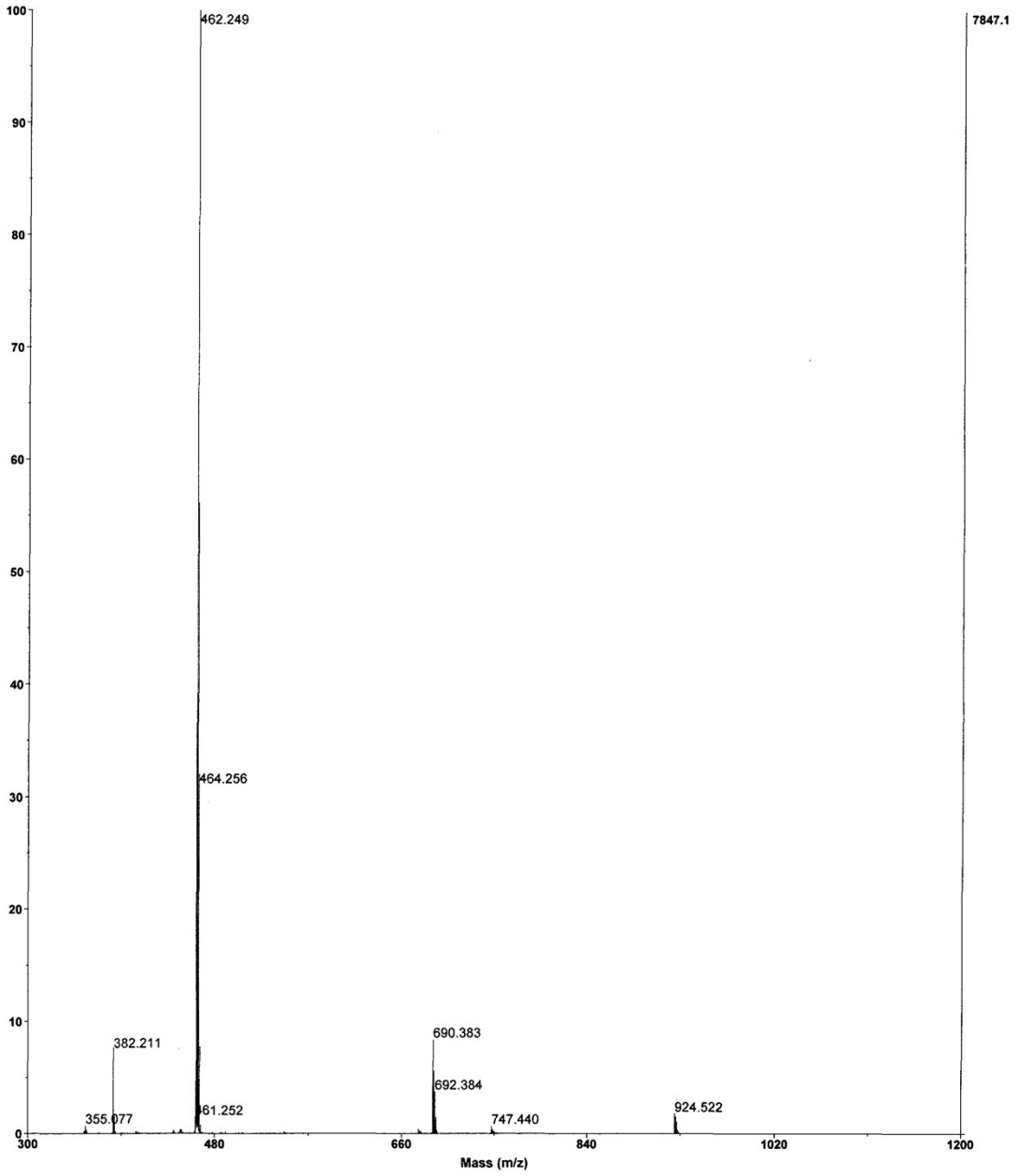

Fig. S2. MALDI-TOF mass spectrum of complex **2**.

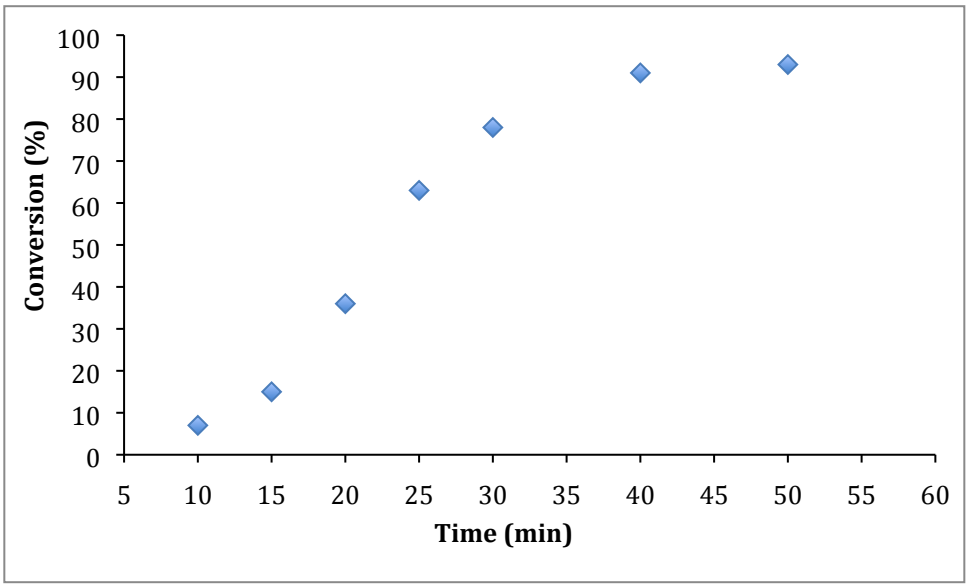

Fig S3. Conversion (%) vs. time for the ROP of *rac*-LA initiated by **1** under the conditions described in Table 1, entry 3.

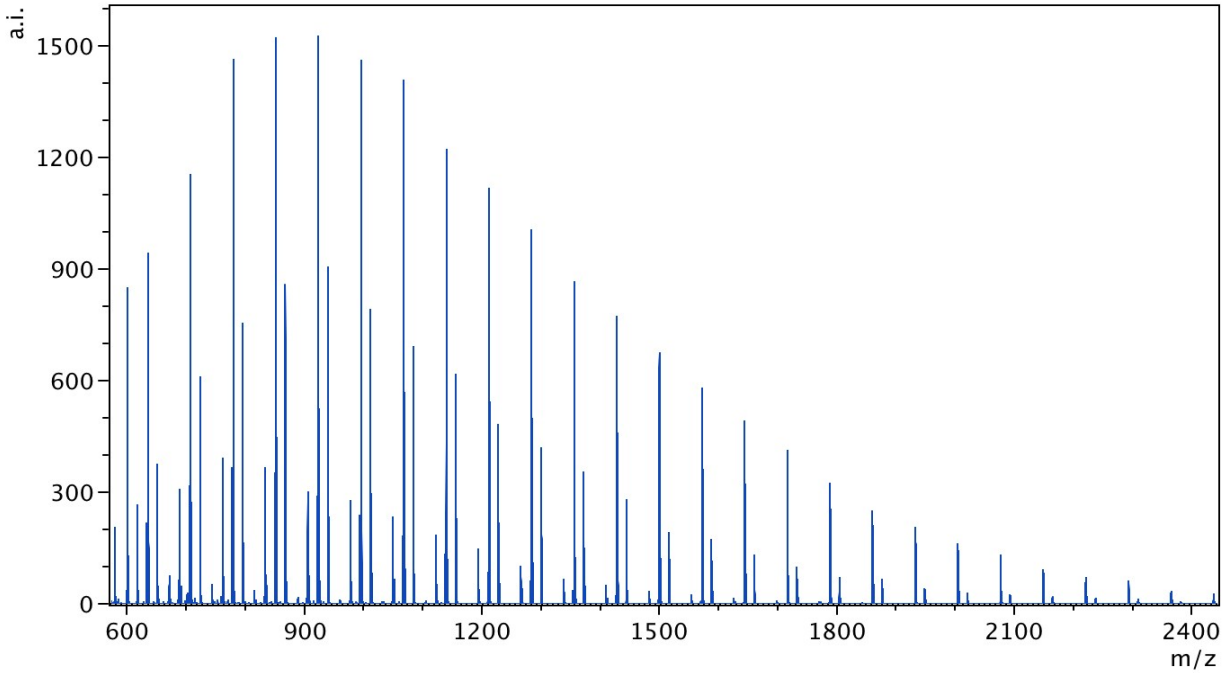

Fig. S4. MALDI-TOF mass spectrum of PLA produced by **1** according to Table 1, entry 1.

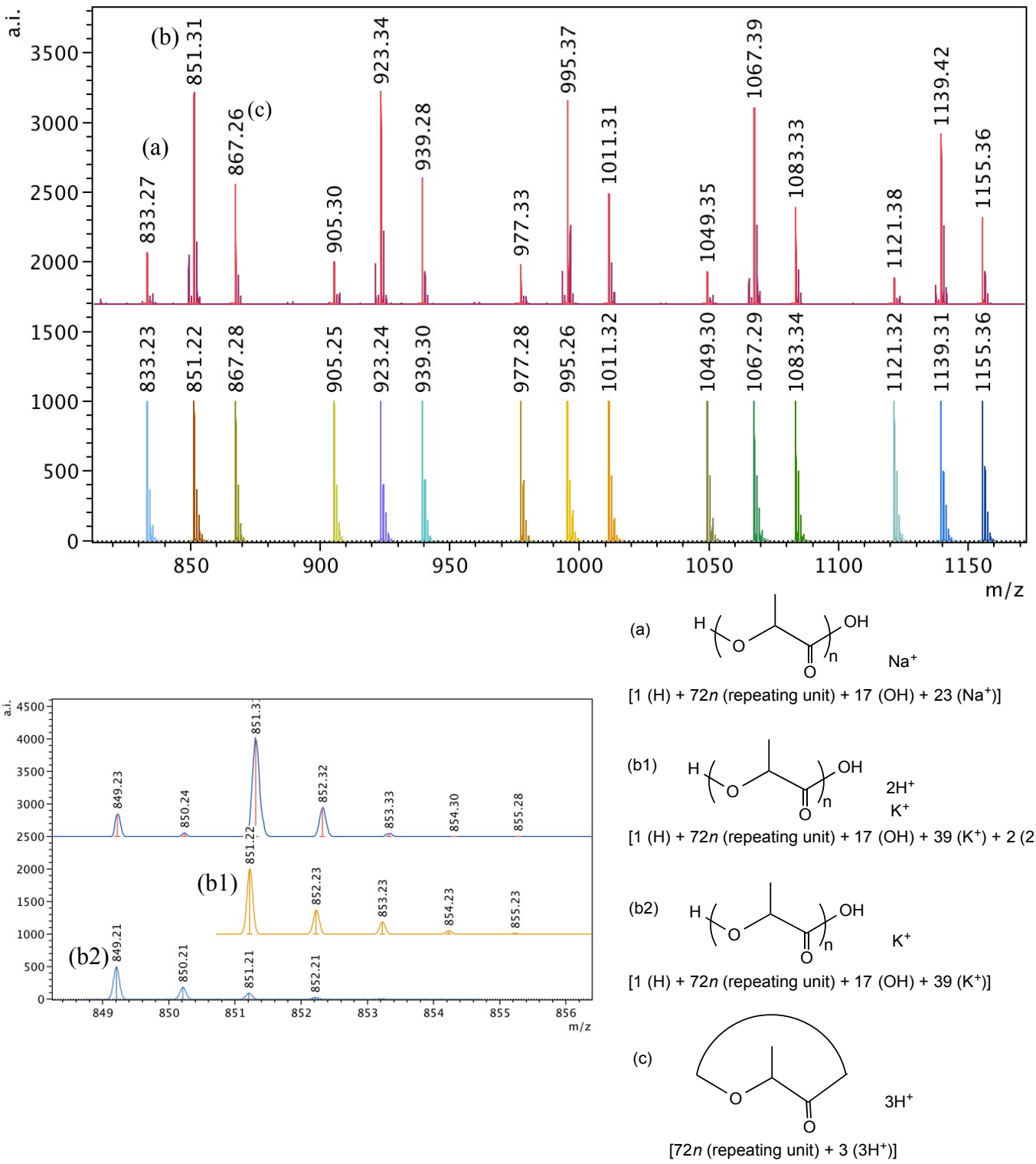

Fig. S5 Top: Expanded region (*m/z* 830 – 1160, n = 54 - 61) of the spectrum with modelled theoretical polymer peaks. Bottom: Expanded region of series (b) with modelled theoretical polymer peaks and possible structures of the polymers based on the calculations shown.

a)  b) 

Fig. S6. Physical appearance of polylactide obtained (a) without BnOH, Table 1, entry 3 and (b) with BnOH, Table 1, entry 4.

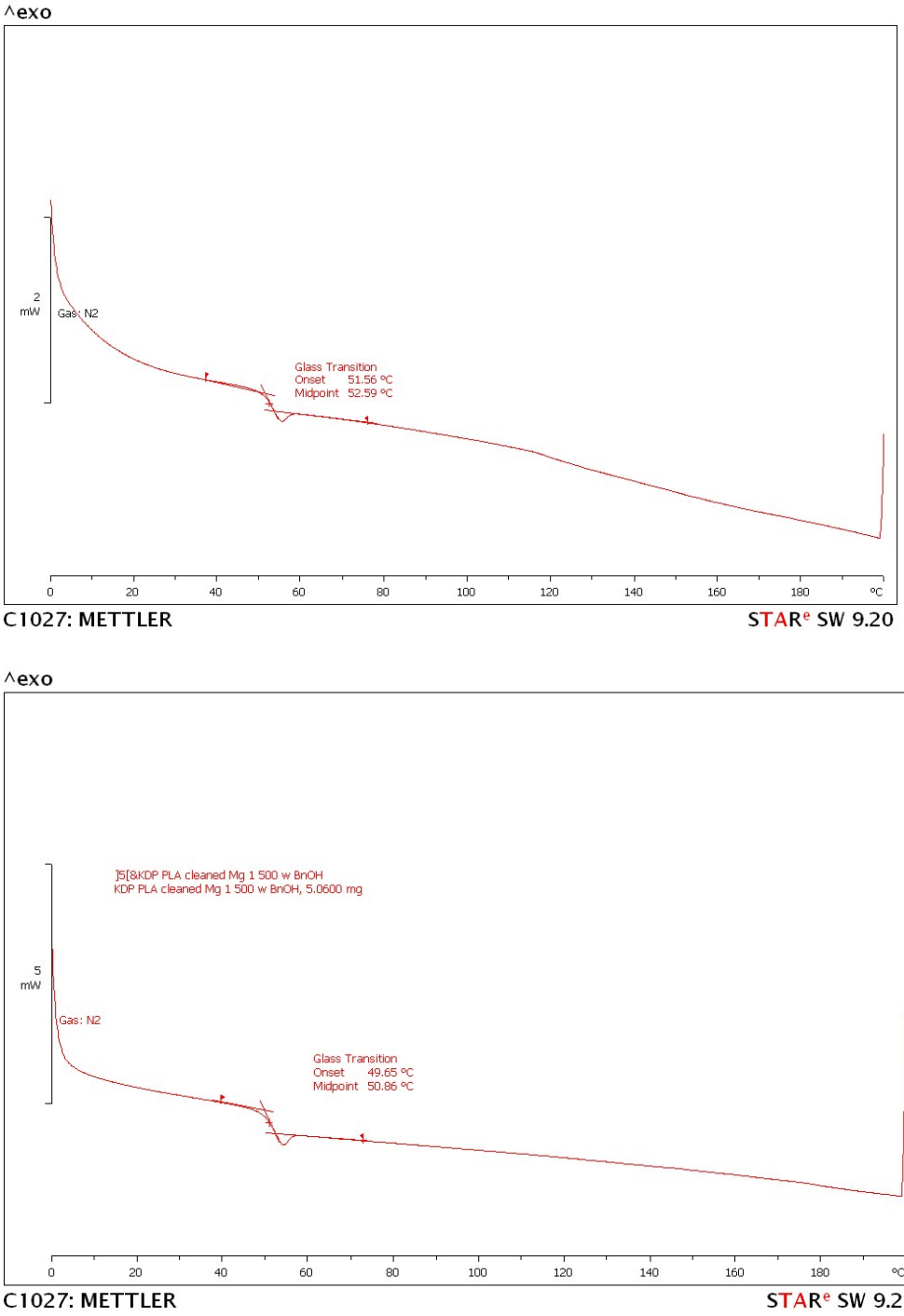

Fig. S7. Top: DSC third heating curve of the polymer obtained using the conditions of Table 1, entry 3 (without BnOH). Bottom: DSC third heating curve of the polymer obtained using the conditions of Table 1, entry 4 (with BnOH).

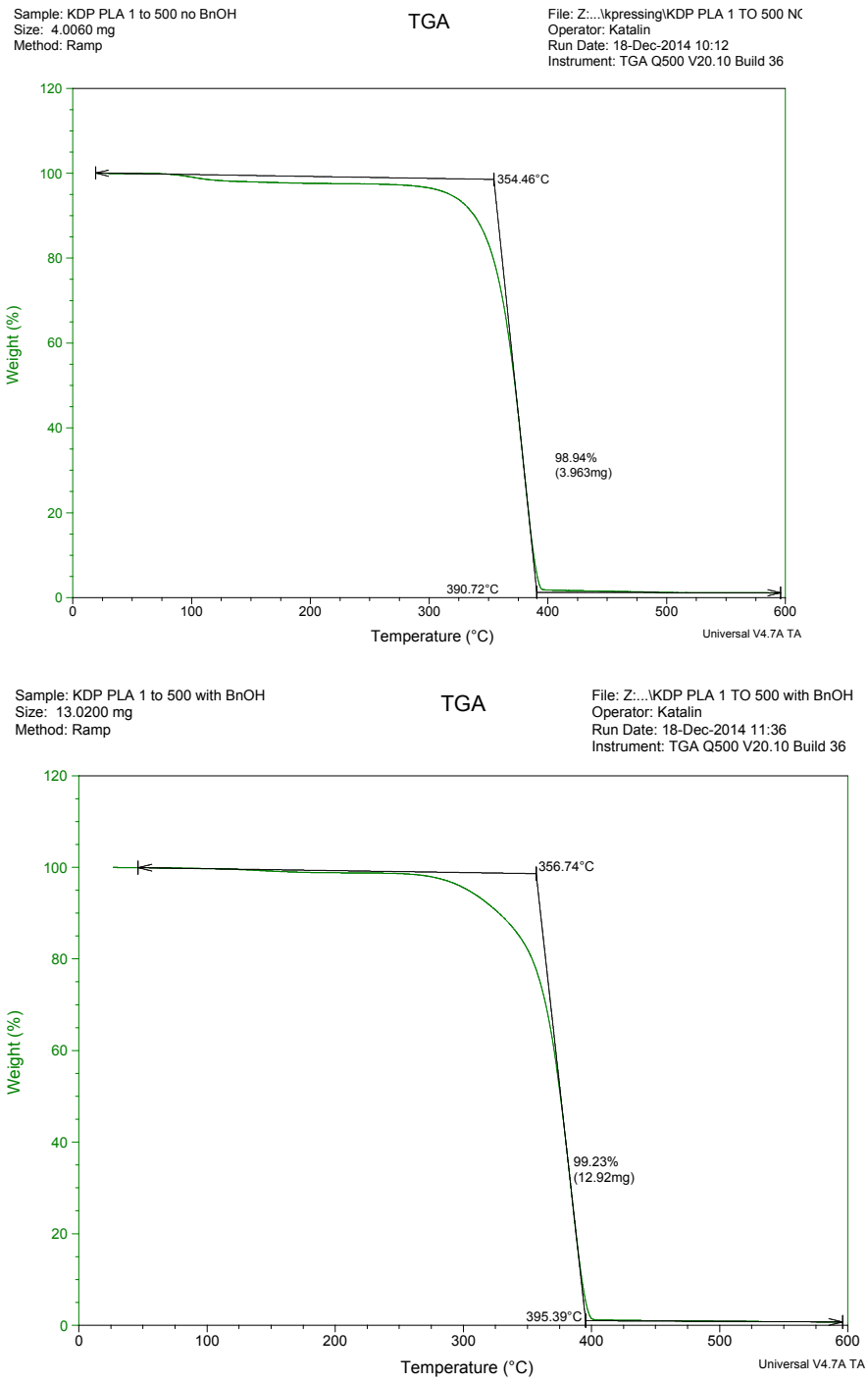

Fig. S8A. TGA curves of polymers obtained, Top: without BnOH using the conditions of Table 1, entry 3. Bottom: With BnOH using the conditions of Table 1, entry 4. Scan rate of 10 °C/min.

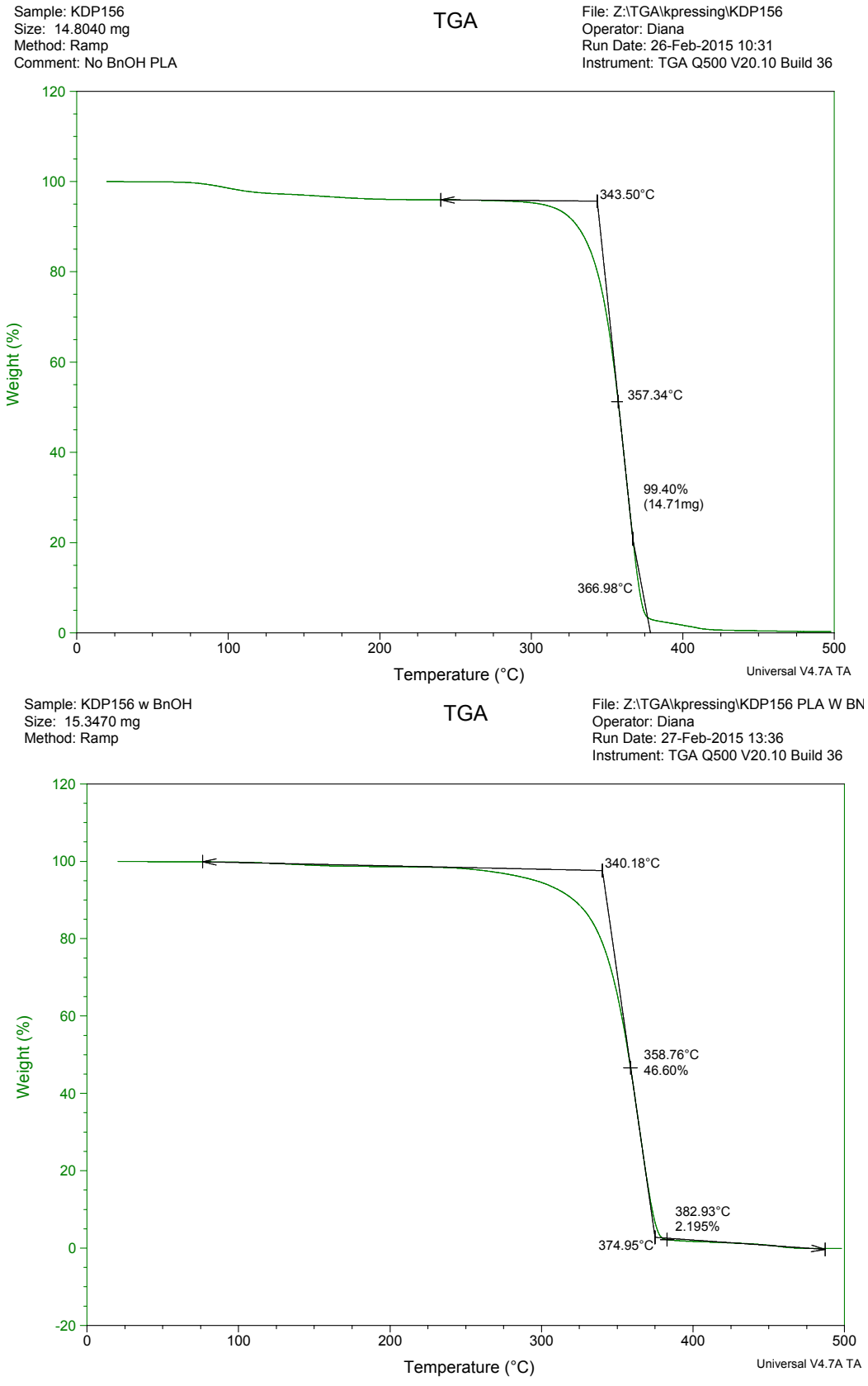

Fig. S8B. TGA curves of polymers obtained, Top: without BnOH using the conditions of Table 1, entry 3. Bottom: With BnOH using the conditions of Table 1, entry 4. Scan rate of 5 °C/min.

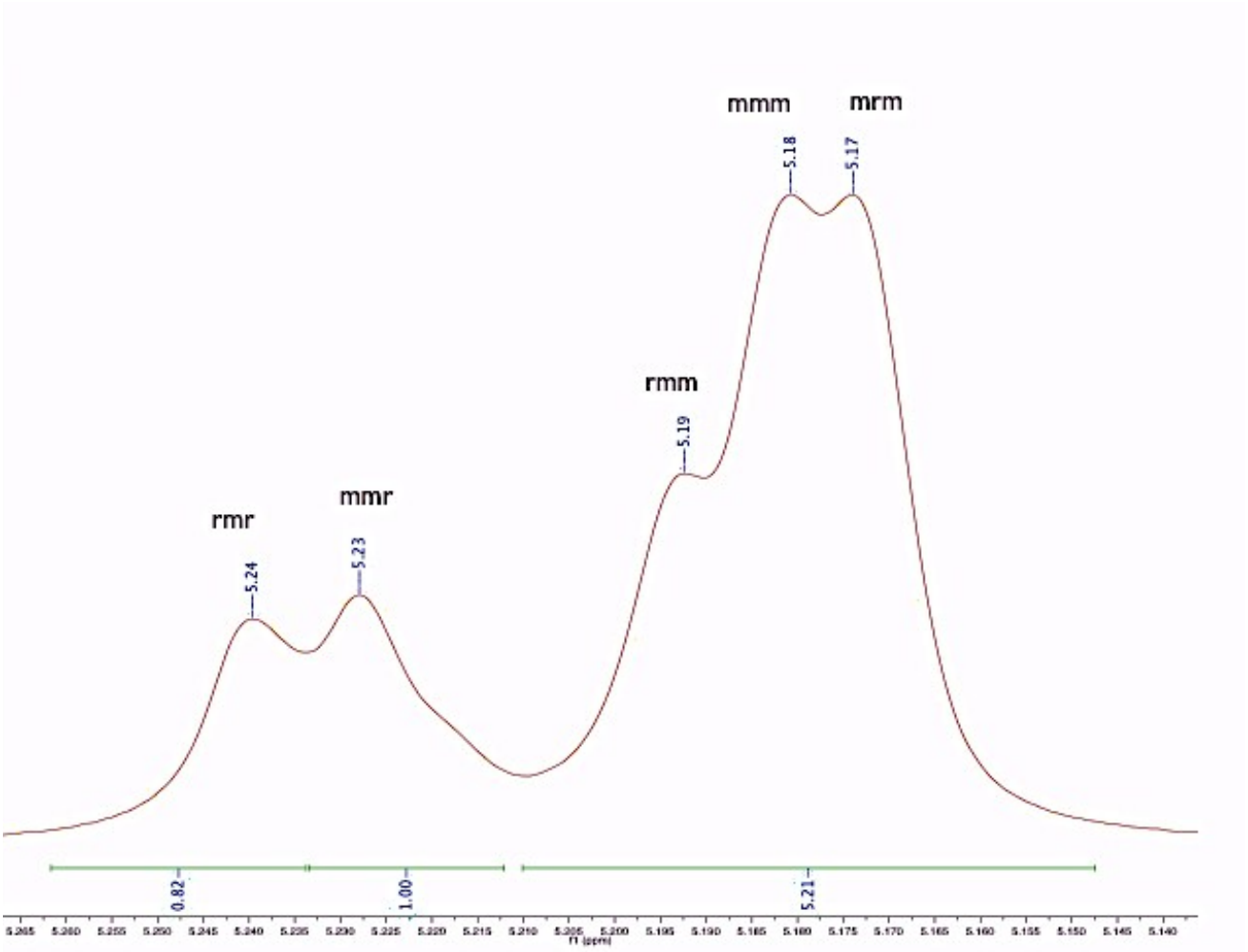

Fig. S9. $^{1}H\{^{1}H\}$-NMR spectrum of the PLA methine region obtained from *rac*-lactide catalyzed by **1** according to conditions in Table 1, entry 1.

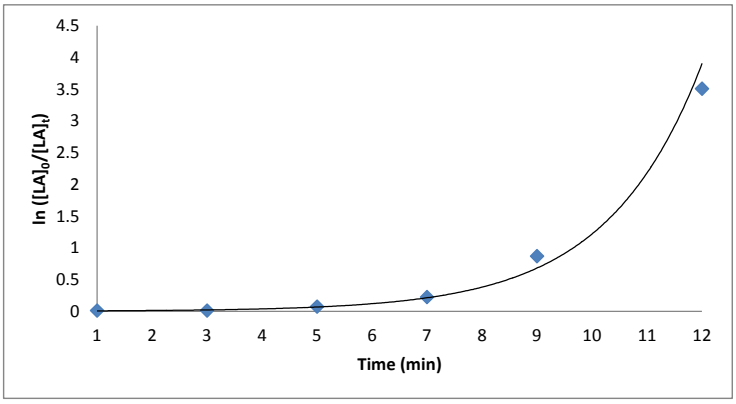

Fig. S10. Plot of $\ln[LA]_0/[LA]_t$ vs. time, $[LA]_0/[Mg]_0$ = 100, in toluene at 90 °C according to the conditions in Table 3, entry 1.

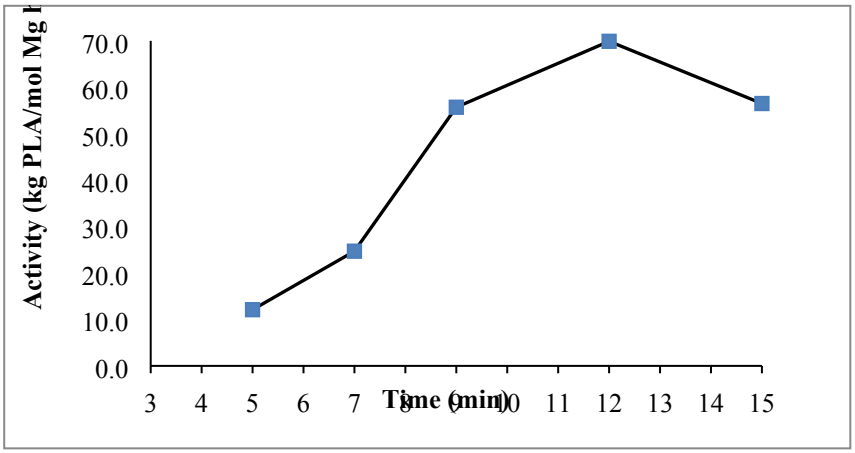

Fig. S11. Activity vs *t* plot for *rac*-lactide ROP according to the conditions described in Table 3, entry 1.

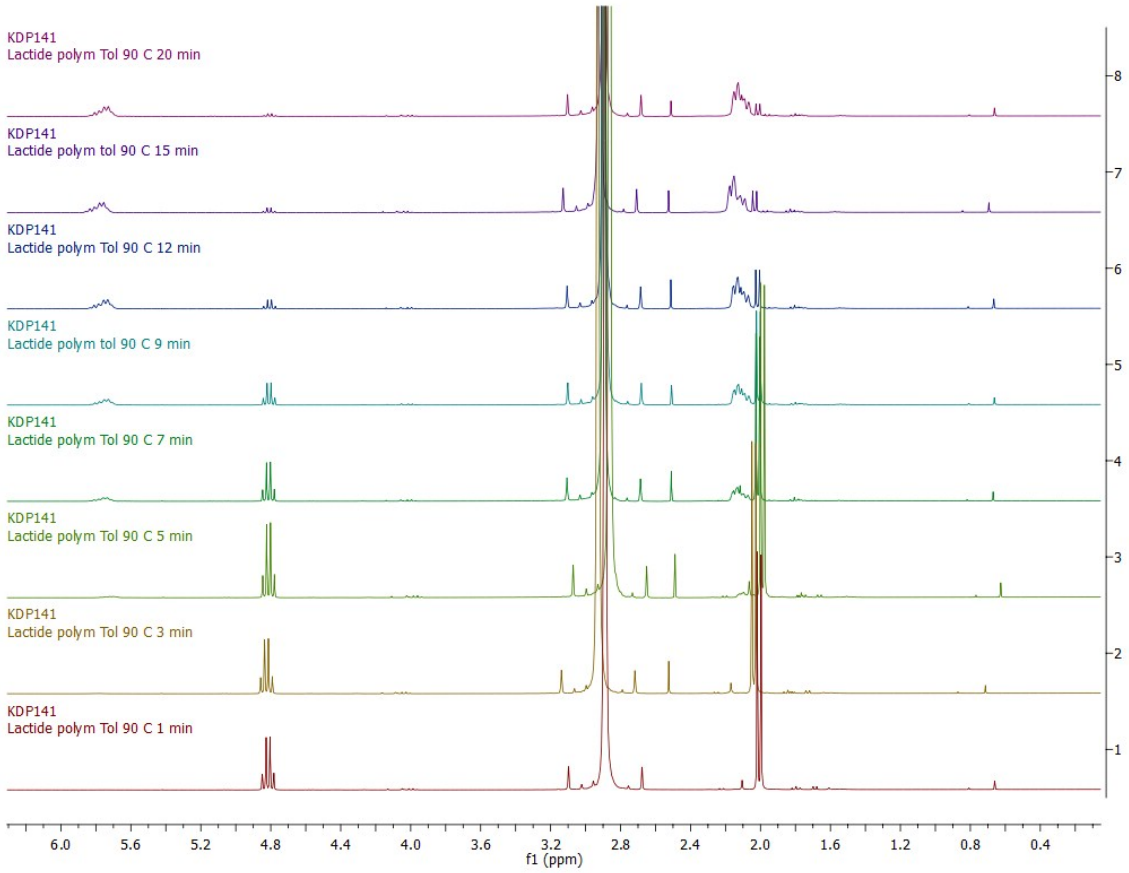

Fig. S12. Stacked ^{1}H-NMR spectra of polymerization of *rac*-lactide by **2** in presence of iPrOH co-initiator ([LA]:[Mg]:[ROH] = 100:1:1) at 90 °C in toluene (Table 3, entry 1).

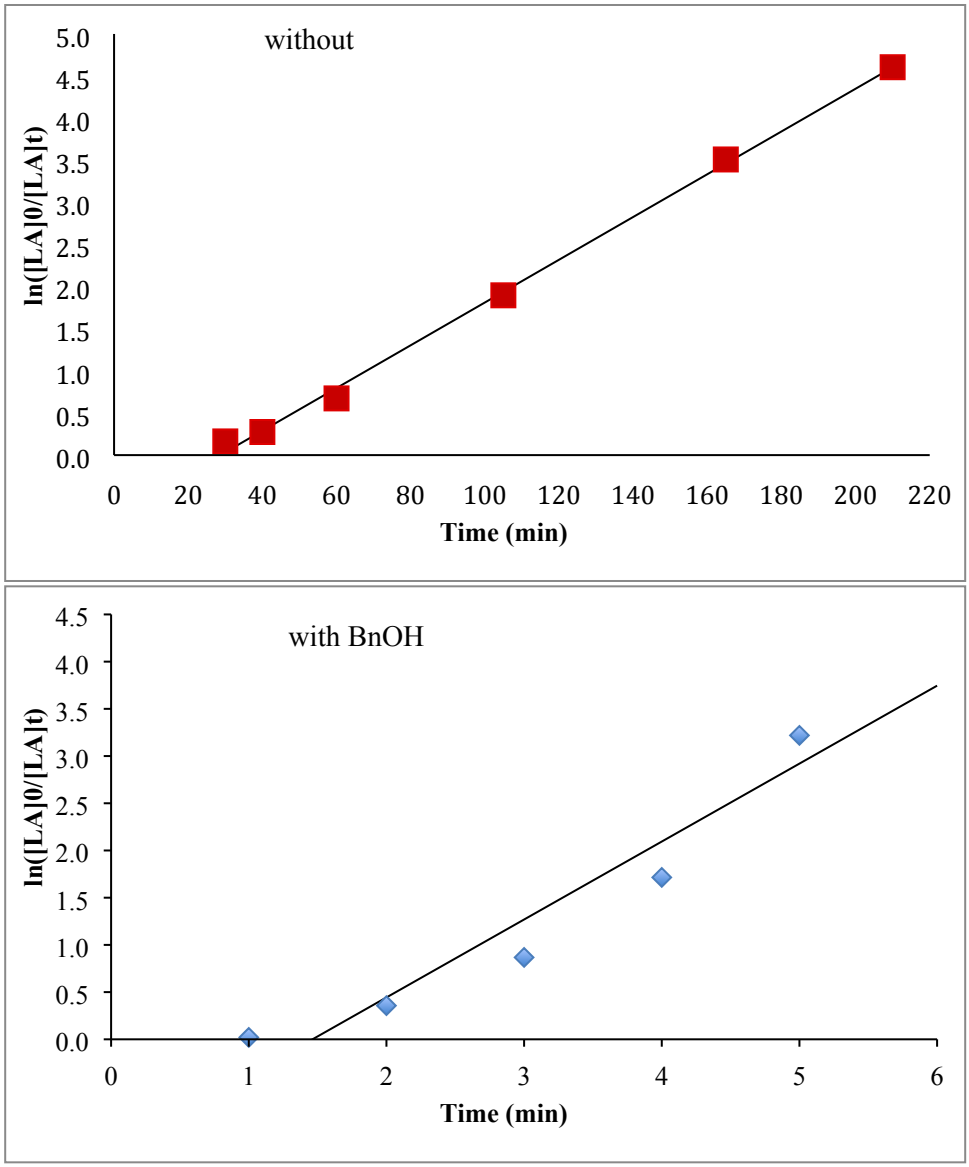

Fig. S13. Plot of $\ln[LA]_0/[LA]_t$ vs. time, $[LA]_0/[Mg]_0 = 100$, in toluene at 90 °C according to the conditions in Table 3, entries 3 (top) and 4 (bottom).

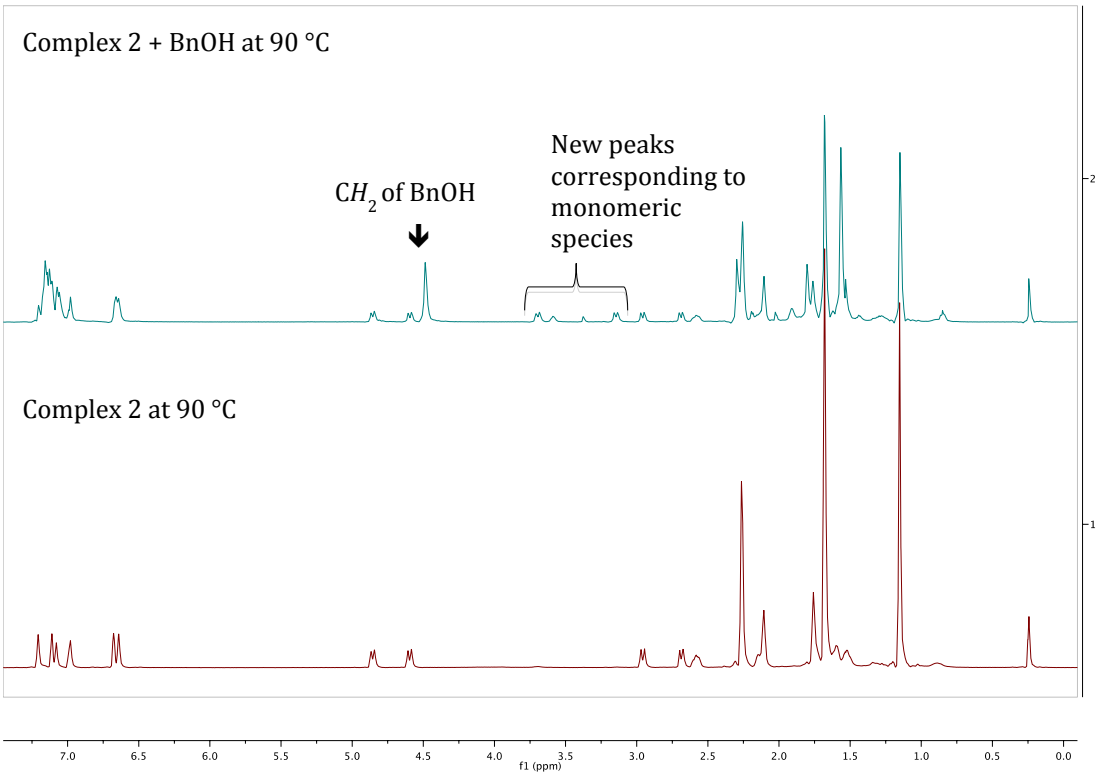

Fig. S14. ^{1}H NMR spectra of complex **2** (bottom) and 1:1 mixture of BnOH co-initiator with complex **2** (top) in toluene-d_8 at 363 K.